energy&fuels

Article

pubs.acs.org/EF

Model for Biomass Gasification Including Tar Formation and Evolution

Carolina Font Palma*,†

School of Chemical Engineering and Analytical Science, The Mill, University of Manchester, Oxford Road, Manchester M13 9PL, United Kingdom

Supporting Information

ABSTRACT: Since tar elimination from the product gas is necessary to make gasification an attractive option, the presence of tar was included in a kinetic model. Lignin was assumed as the main precursor of tars due to its aromatic nature; therefore, the lignin content of biomass was considered as part of the fuel characterization. This work shows the results from the simulation of the fluidized bed gasifier that incorporates the proposed mechanism for tar formation and evolution into the kinetic model. Model results were compared with experimental data from wood gasification. The comparison showed that the model was consistent with what was expected during the evolution of primary tars according to experimental work from previous reports. However, the model overestimated tars of class 2 and the total tar concentration.

1. INTRODUCTION

Tar is a complex mixture of condensable hydrocarbons comprising single-ring to five-ring aromatic compounds plus other oxygen-containing hydrocarbons and complex polycyclic aromatic hydrocarbons (PAH) produced during thermochemical conversion processes.[1] The presence of tar can cause operational problems and may condense on cooler surfaces downstream which can lead to blockage of particle filters and of fuel lines. Therefore, the ultimate goal to make gasification an attractive option is tar elimination from the product gas.

Due to the complexity of tar, most reports are mainly concerned with identification and quantification of PAH from pyrolysis or combustion.[2] In the case of kinetic studies, focus has been given to determination of either kinetic parameters for the overall weight loss of the fuel or kinetic parameters for evolution of light gases (such as CO, CH_4, and H_2). As a result, there are still insufficient kinetic data and theoretical comprehension of the tar reaction process during gasification.

Tars are normally modeled as a "lump" or using the most stable components such as toluene, naphthalene,[3] benzene, and phenol;[4] however, these species are known to appear as secondary and/or tertiary tars, and the mechanisms and kinetics of their formation are often omitted. On the other hand, a detailed kinetic model for lignin devolatilization that includes as much as 100 species becomes a complex problem when being incorporated to simulate conversion of biomass inside the gasifier. The kinetic model used three reference lignin units to represent the initial lignin structure, 100 molecular and radical species were involved in the mechanism, and the mass balances included the net rate of formation.[5] Good model predictions were obtained when compared to experimental thermogravimetric analysis (TGA) data from a variety of pyrolyzed lignins.

On the basis of identification of tar compounds from experimental work, the most frequent individual tar species studied experimentally and as model tars are acetol, acetic acid and guaiacols (primary tars),[6,7] phenols, cresols and toluene (secondary tars),[8] and naphthalene (tertiary tar).[9] A mechanism that could describe formation of tars while maintaining a minimum number of tar species represents a more practical solution for tar simulation during biomass gasification. The objective of this work is to present a model that includes a proposed mechanism for tar formation and evolution for a fluidized bed gasifier. The model is based on the findings from a previous publication of a review of the work on tar formation and evolution during biomass gasification.[10] The findings of the review were used as a framework for the present model which will include a mechanism for tar formation and evolution.

2. THEORETICAL BACKGROUND FOR TAR REACTION MECHANISM

Biomass composition comprises lignin, cellulose, and hemicellulose. Lignin fraction normally consists of 20−40 wt % dry of biomass.[11] Since only the lignin fraction of the biomass is aromatic in nature, lignin is assumed as precursor for PAH formation in this work.

A mechanism that incorporates tar formation is presented, and its development consisted of two steps. First, a list of the main tar compounds was made based on the tar compounds identified as most abundant from the literature after running biomass pyrolysis experiments. Second, possible reaction pathways were evaluated by selection of the most favorable reactions to occur in the process based on thermodynamics; reactions evaluated are provided in the Supporting Information.

Catechol (1,2-dihydroxybenzene), guaiacol (2-methoxyphenol), and vanillin (4-hydroxy-3-methoxybenzaldehyde) were chosen to represent primary tar products in the present work according to the typical structure of lignin. Guaiacol and vanillin were selected because previous reports have shown that these two guaiacols are dominant products during biomass pyrolysis,[2,6,12] and lignin is rich in methoxyl groups ($-OCH_3$). Catechol was chosen because it is a predominant unit in lignin and coal as well as present in biomass tars. Other researchers have used catechol and dihydric phenol catechol as model compounds of lignin units.[7]

In this work, lignin is represented by seven guaiacol, seven vanillin, and two catechol units. The 16 units are put together and

Received: March 11, 2013
Revised: April 11, 2013
Published: April 11, 2013

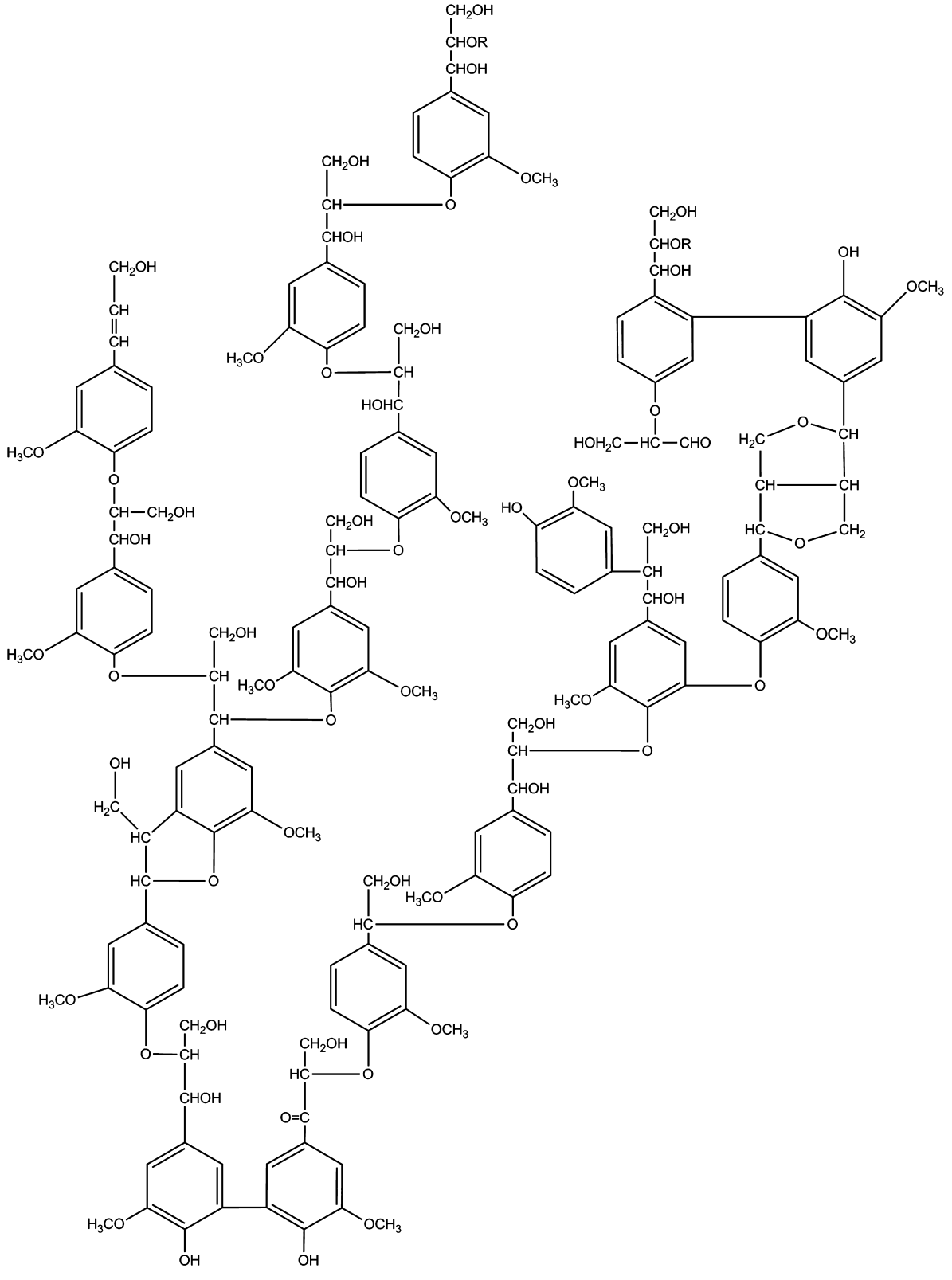

Figure 1. Typical structure of a softwood lignin.[5,13]

accounted for 70% of the softwood lignin proposed by Adler[13] shown in Figure 1. The main assumptions were that

- only the lignin fraction is aromatic in nature,
- the main route for soot formation is via tar components reactions, and
- formation of cyclopentadiene and indene intermediates are responsible for PAH growth.

Figure 2 shows the proposed mechanism for tar formation assuming lignin units as precursors. The three lignin units, vanillin ($C_8H_8O_3$), guaiacol ($C_7H_8O_2$), and catechol ($C_6H_6O_2$),

dx.doi.org/10.1021/ef4004297 | *Energy Fuels* 2013, 27, 2693−2702

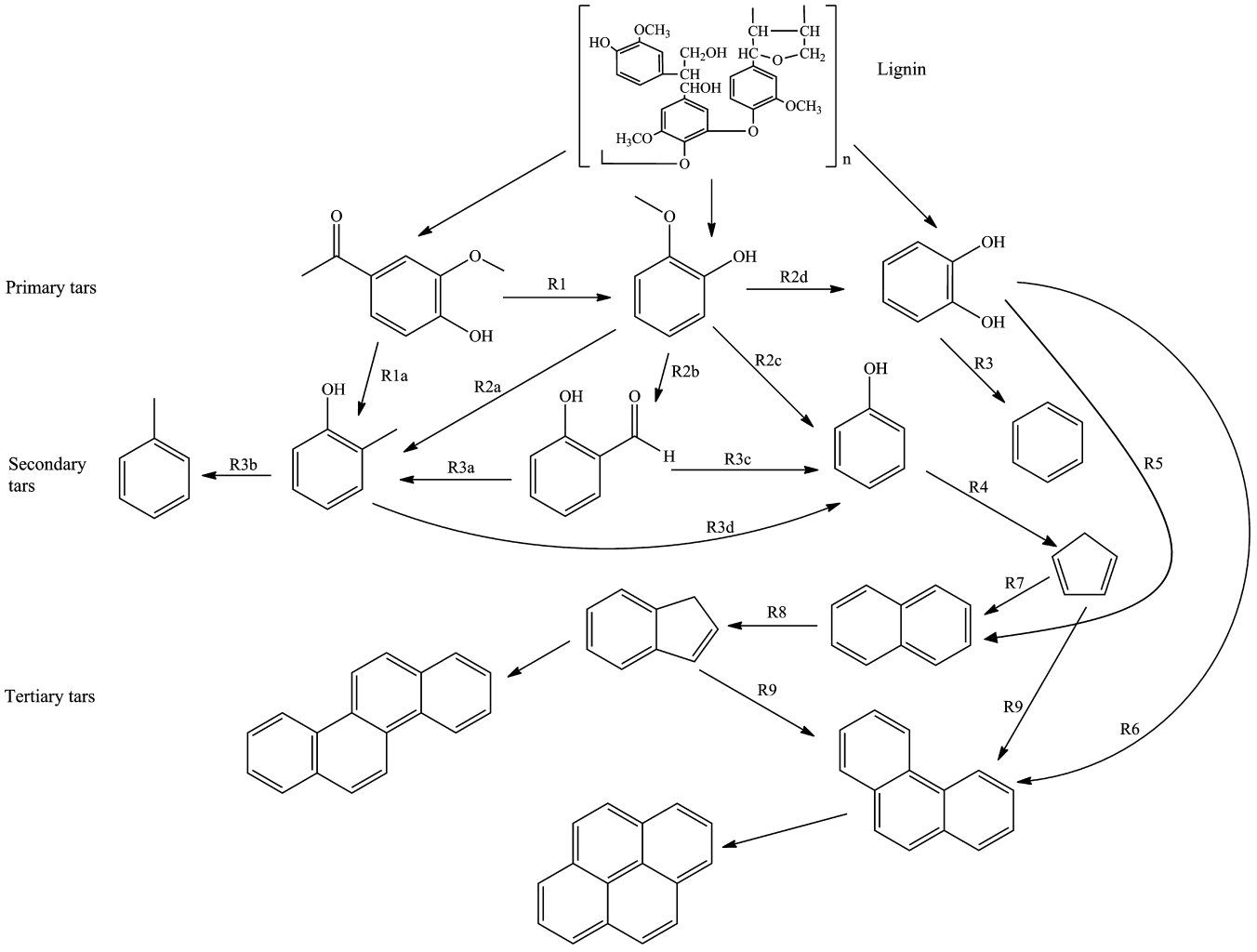

Figure 2. Proposed mechanism for primary, secondary, and tertiary tar formation.

are pyrolyzed and/or react with hydrogen. This figure does not show release of volatiles, such as CO, H_2, and CO_2, which are also produced. The reaction pathway was chosen according to reactions that were most thermodynamically favorable. Reaction R1 represents reaction of vanillin pyrolysis, and reaction R1a is reaction of vanillin with hydrogen. For example, reaction *R3c* was not included in the model; this reaction might also occur, but it was not considered because it is not thermodynamically favorable (see Supporting Information). Phenol is transformed to cyclopentadiene, and CO is abstracted from the phenol according to reaction R4. Afterward, cyclopendiene combines to form naphthalene in accordance with reaction R7.

3. MODEL

The kinetic model consists of a bubbling fluidized bed with sand particles and on top a freeboard zone. Air is used as gasifying agent and previously preheated. A schematic diagram of the fluidized bed is shown in Figure 3. The model assumptions are

- steady-state regime,
- one-dimensional fluidized bed, where variations in conditions occur only in the axial z direction,
- two-phase model for the hydrodynamic behavior of the fluidized bed, where gas flow entering the reactor at u_0 velocity is divided into two phases, the emulsion phase and the bubble phase,
- solids in the bed are well mixed inside the emulsion phase,

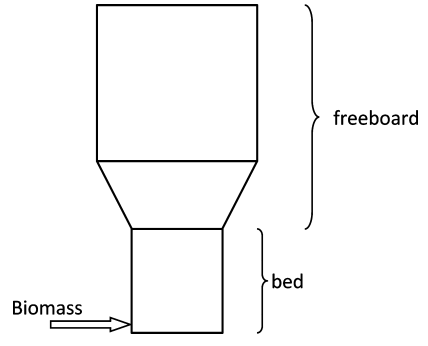

Figure 3. Schematic diagram of the fluidized bed.

- the bed consists of sand, ash, and carbon,
- biomass devolatilization occurs instantaneously since mixing of biomass particles proceeds more slowly than pyrolysis;[14] therefore, biomass pyrolysis takes place on entry to the bed. The lignin fraction undergoes primary pyrolysis along the bed zone,
- homogeneous and heterogeneous reactions occur in the emulsion phase, since it contains all particles and a portion of the gases. Gases are maintained at minimum fluidization conditions, and excess gas passes through the bed to the bubble phase,

dx.doi.org/10.1021/ef4004297 | *Energy Fuels* 2013, 27, 2693−2702

Table 1. Homogeneous and Heterogeneous Reactions

reaction	ref
$C_8H_8O_3 \rightarrow C_7H_8O_2 + CO$ (R1)	16
$0.705C_7H_8O_2 \rightarrow 0.47C_6H_6O_2 + 0.04C_6H_6O + 0.07C_7H_8O + 0.15C_7H_6O_2 + 0.275CH_4 + 0.06CO + 0.01H_2$ (R2)	17
$C_6H_6O_2 + 2H_2 \rightarrow C_6H_6 + 2H_2O$ (R3)	7
$C_6H_6O \rightarrow C_5H_6 + CO$ (R4)	18
$2C_6H_6O_2 \rightarrow C_{10}H_8 + 2CO_2 + 2H_2$ (R5)	7
$3C_6H_6O_2 \rightarrow C_{14}H_{10} + 4CO + 2H_2O + 2H_2$ (R6)	7
$2C_5H_6 \rightarrow C_{10}H_8 + 2H_2$ (R7)	19
$C_{10}H_8 + O_2 \rightarrow C_9H_8 + CO_2$ (R8)	19
$C_9H_8 + C_5H_6 \rightarrow C_{14}H_{10} + 2H_2$ (R9)	20
$C + 0.5O_2 \rightarrow CO$ (R10)	21
$CO + 0.5O_2 \rightarrow CO_2$ (R11)	22
$H_2O_l \rightarrow H_2O_g$ (R12)	23
$CO + H_2O \rightarrow CO_2 + H_2$ (R13)	24
$H_2 + 0.5O_2 \rightarrow H_2O$ (R14)	21
$C + H_2O \rightarrow CO + H_2$ (R15)	24
$C + 2H_2 \rightarrow CH_4$ (R16)	24
$CH_4 + H_2O \rightarrow CO + 3H_2$ (R17)	25
biomass $\rightarrow a_1CO + a_2CO_2 + a_3H_2O + a_4H_2 + a_5CH_4 + a_6NH_3 + a_7H_2S + a_8HCl + a_9$char (R18)	
$2H_2S + 3O_2 \rightarrow 2SO_2 + 2H_2O$ (R19)	26
$NH_3 + 5/4O_2 \rightarrow NO + 3/2H_2O$ (R20)	27
lignin $\rightarrow 2C_6H_6O_2 + 7C_7H_8O_2 + 7C_8H_8O_3$ (R21)	
$Na_2CO_3 + 2HCl \rightarrow 2NaCl + CO_2 + H_2O$ (R22)	28
$C_8H_8O_3 + 6.68H_2 \rightarrow 2.66CO + 0.085CO_2 + 5.255CH_4 + 0.17H_2O$ (R23)	24
$C_{10}H_8 + 4H_2O \rightarrow C_6H_6 + 4CO + 5H_2$ (R24)	29
$C_6H_6 + 3O_2 \rightarrow 6CO + 3H_2$ (R25)	21
$C_6H_6 + 5H_2O \rightarrow 5CO + 6H_2 + CH_4$ (R26)	3
ash $\rightarrow$ ash (R27)	

- only homogeneous reactions occur in the bubble phase, since it is considered as free of particles,
- all gases in both phases are assumed as in plug flow mode,
- mass transfer between bubble and emulsion phases occurs through molecular diffusion. Mass transfers in the axial or vertical direction within each phase are considered as negligible compared to transfers in the horizontal direction between phases,
- energy balance considers heat of reaction, heat exchange between bubble and emulsion phases, and heat exchange between well-mixed particles and gas in the emulsion phase, and
- the gases that travel to the freeboard zone are assumed in plug flow mode.

Hydrodynamics of the fluidized bed, rate of reactions for homogeneous and heterogeneous reactions, and mass transfer between emulsion and bubble phases were considered. For the carbonaceous material, a global mass balance is integrated over the gasifier bed zone. For the freeboard region, it is considered that homogeneous reactions continue as it was a second reactor in series with the fluidized bed. Equations of mass and energy balances for the emulsion phase, bubble phase, carbonaceous material, and freeboard zone can be found in the Supporting Information.

Table 1 shows the reactions used in the kinetic model, and kinetics are provided in the Supporting Information. Reaction R18 represents flash pyrolysis of biomass that releases volatiles, i.e., noncondensable gases and water and char. Biomass composition is based on the ultimate analysis minus the lignin ultimate analysis. Char was assumed as only composed of carbon.

Reaction R21 corresponds to formation of primary tars, the three lignin units previously chosen, vanillin, guaiacol, and catechol. Evolution of these three tars followed the mechanism shown in Figure 2, which corresponds to reactions R1−R9. Reactions R10−R17, R19, and R20 represent combustion and gasification reactions of carbon and volatiles.

Reactions R18 and R21 represent the primary decomposition of biomass based on a one-component reaction process. This approach is normally adopted for fast heating rates, and kinetics are derived from yield measurements and weight-loss curves of the three product classes (gases, tar, and char) formed.[15] The mechanism was chosen as two parallel reactions occurring for

dx.doi.org/10.1021/ef4004297 | Energy Fuels 2013, 27, 2693−2702

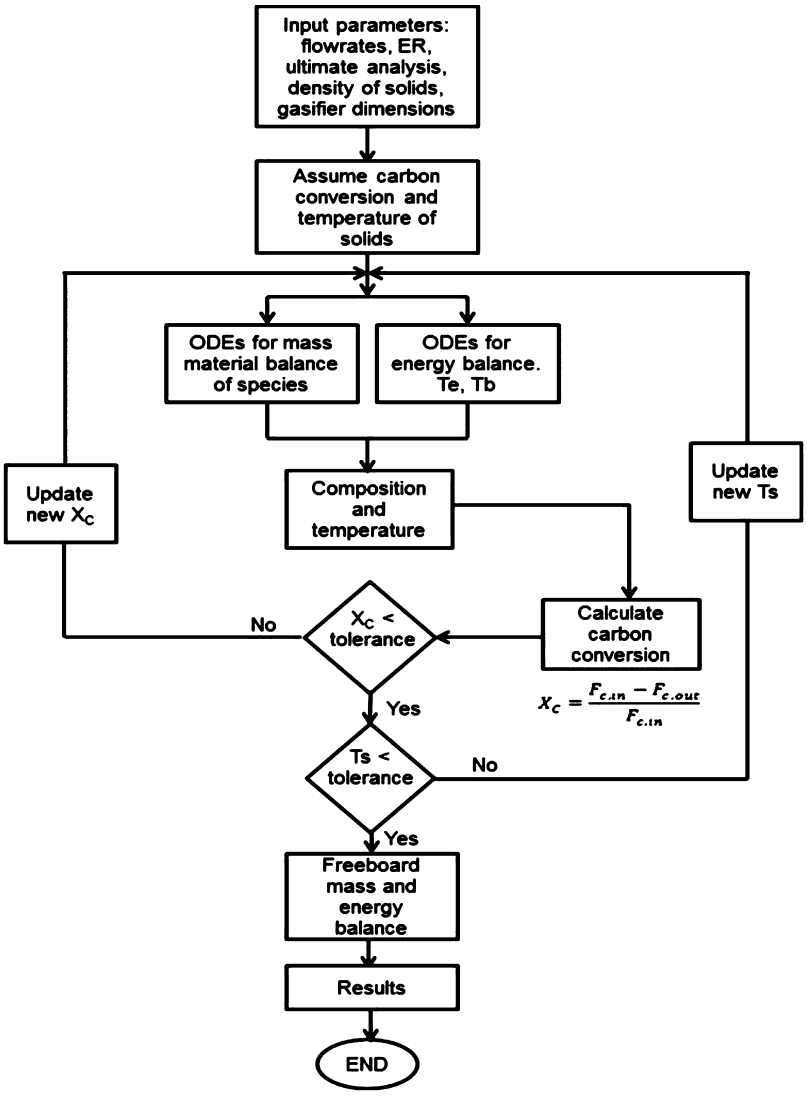

Figure 4. Flow diagram of the model for the fluidized bed gasifier.

formation of the three product classes. After these three product classes are produced, they are further decomposed and underwent combustion and gasification reactions.

For the rates of reaction of catechol, kinetic parameters and reaction order were taken from work on the pyrolysis of catechol. The kinetics parameters for reactions R3 and R5 were taken from Ledesma et al.[7] In Ledesma et al.'s work, experimental product yield/temperature data and observed maximum yields were fitted to obtain the activation energy and pre-exponential factor for each product species when a first-order reaction was assumed, at a fixed residence time. Individual kinetics for some benzene and benzenoid PAH, vinyl- and ethyl-substituted aromatics, and cyclopenta-fused PAH compounds were derived.

Reaction R23 shows the decomposition of vanillin to non-condensable gases and water. Reaction R24 corresponds to steam gasification of naphthalene. Reactions R25 and R26 represent combustion and steam gasification of benzene, respectively.

Ash was assumed to contain a fraction of sodium carbonate; the rest was considered as inert. Reaction R22 represents reaction of Na_2CO_3 with HCl to retain chlorine in the solid phase.

For the solution of mass equations of individual species (eqs 1 and 3, Supporting Information) and energy equations (eqs 2 and 4, Supporting Information) from the Supporting Information, a generalization of the Runge–Kutta method, the Rosenbrock method was used to solve the set of stiff ODEs, where initial conditions at the bottom of the gasifier were given and concentrations were calculated up top of the fluidized bed and freeboard zone. The NAGWare f95 Compiler was selected for coding the model, which is a full ISO and ANSI standard implementation of the FORTRAN 95 language. The LU decomposition (direct method) was performed using the NAG Fortran Library Routine F01BRF for a real sparse matrix.

Figure 4 shows a schematic diagram of the simulation program coded in Fortran. Two iteration processes were used: one iteration was concerned with carbon conversion and the other with the temperature of solids. Input parameters that consist of air flow rate, biomass flow rate, temperature of air, gasifier dimensions, density of solids, particle size, ultimate analysis, lignin content, and moisture content were provided to start simulations. Carbon conversion and temperature of solids were given as an initial guess. The Rosenbrock method was used to solve the ODEs and obtain the temperatures and composition of the different phases. The solid reaction rate was integrated over the bed height using eq 5 from the Supporting Information, and the new carbon conversion was obtained and compared with the initial guess. Once the carbon fraction iteration finished, the

dx.doi.org/10.1021/ef4004297 | *Energy Fuels* 2013, 27, 2693–2702

energy equation of the solid was integrated using eq 6 from the Supporting Information, and a new temperature of the solid was obtained and then compared with the initial guess.

4. RESULTS AND DISCUSSION

In order to verify the results generated from the kinetic model, experimental data was taken from the work conducted in a lab-scale bubbling fluidized bed gasifier of the Energy Research Centre of The Netherlands (ECN).[30] The fuel employed was beech chips, and Table 2 shows the properties of the beech used during the gasification experiments.

Table 2. Properties of Fuel (as received)[30]

	beech wood
ultimate analysis (wt %, dry)	
carbon	48.55
hydrogen	5.97
nitrogen	0.14
sulfur	0.017
oxygen	44.28
chlorine	0.005
ash	1.04
proximate analysis (wt %, dry)	
fixed carbon	16.0
volatile matter	83.0
moisture	10.2
lignin	24.0
HHV (kJ/kg)	19 071

The gasifier was configured to be heated electrically in order to control the gasifier temperature. The temperatures of bed and freeboard were recorded, and noncondensable gases (CO, CO_2, CH_4, H_2, C_2H_4, and C_2H_6), benzene, and toluene were measured online by GC-MS and other tars offline using solid-phase absorption (SPA). Table 3 shows the gasifier and bed material characteristics.

Table 3. Fluidized Bed Characteristics[30]

parameter	
bed material	silica sand
particle diameter	0.27 mm
bed internal diameter	74 mm
bed height	500 mm
freeboard diameter	108 mm
total length	1100 mm
gasifying agent	air

Model Verification. Table 4 shows a comparison of the results reported from experimental work with the kinetic model results using the operating conditions indicated in the table, such as fuel feeding rate. Results are shown using two equivalence ratio (ER) values. The table compares experimental and predicted product gas compositions, bed and freeboard operating temperatures, and total tar and tars compositions.

The results of tar compounds were reported according to the tar classification system. Class 1 refers to GC-undetectable tars, like heaviest tars that condense at high temperatures even at low concentrations. Class 2 refers to heterocyclic compounds that generally have high water solubility, such as phenol and cresol. Class 3 includes 1-ring aromatic compounds, for example, xylene, styrene, and toluene. Class 4 refers to 2−3-ring PAH compounds, such as naphthalene, flourene, and phenanthrene. Class 5 includes higher PAH compounds, that is, 4−7-ring aromatic compounds from fluoranthene to coronene.[31]

Table 4. Comparison between Experimental[30] versus Kinetic Results of Beech Gasification

	units	exp. data	kinetic model	exp. data	kinetic model
ER		0.25	0.25	0.26	0.26
biomass feeding rate	kg/h	1	1	1	1
CO	vol %	14.09	12.9	14.20	13.4
CO_2	vol %	13.25	13.7	13.18	13.5
H_2	vol %	7.17	9.1	7.10	8.8
N_2	vol %	43.04	57.5	43.94	58.4
CH_4	vol %	4.22	0.54	4.23	0.37
H_2O	vol %	15.6[a]	5.4	15.5[a]	4.9
SPA total tar	g/m^3	10.0	21.0	7.6	13.7
class 2	mg/m^3	1089	17255	471	10 909
class 3	mg/m^3	1359	1871	756	1481
class 4	mg/m^3	5495	1876	5024	1342
phenol	mg/m^3	1015	555	425	339
class 5	mg/m^3	311		354	
temperature bed	K	1079	969	1103	965
temperature freeboard	K	1049	910	1073	918
temperature of air	K	298	960	298	967
carbon conversion	%	97−99	96.7	97−99	97.0

[a]Calculated.[30]

In order to compare the predicted results with the experimental data, tar concentrations were presented by grouping the simulated tar compounds according to the tar classification system. Vanillin, guaiacol, catechol, phenol, *o*-cresol (2-methylphenol), and salicylaldehyde (2-hydroxybenzaldehyde) were counted as class 2. Cyclopentadiene and benzene were considered class 3. Finally, naphthalene, indene, and phenanthrene were added as class 4. Class 5 was not reported since aromatic compounds of four or more rings were not considered in the model.

Results from the kinetic model showed that the concentration of class 2 was much higher than expected. This high concentration was mainly due to catechol and salicylaldehyde, where only adding these two compounds gave a concentration of 14.7 and 9.2 g/m^3 with an ER of 0.25 and 0.26, respectively. One of the limitations of the proposed set of reactions is that combustion reactions of catechol and salicylaldehyde and pyrolysis and gasification of salicylaldehyde were not included due to lack of kinetics. These two compounds were generated from pyrolysis of guaiacol, which is a primary tar. This reaction caused decomposition of guaiacol while producing primary tar catechol and secondary tar salicylaldehyde among others, according to reaction R2 as shown in section 3.

Another difference between the results presented in Table 4 of the predicted and experimental data was the temperatures of inlet air and gasifier. This difference was due to the fact that the fluidized bed gasifier from ECN had electrical heaters to control the temperature of the bed and freeboard to particular values. In contrast, the model assumes introducing hot air to achieve high temperatures in both sections. In order to improve the comparison, the model would need to be adjusted to include the option of choosing that the gasifier is externally heated to maintain or achieve certain temperature.

Even though it was observed that the increase of air temperature helped to reduce tar production, the air temperature

dx.doi.org/10.1021/ef4004297 | Energy Fuels 2013, 27, 2693−2702

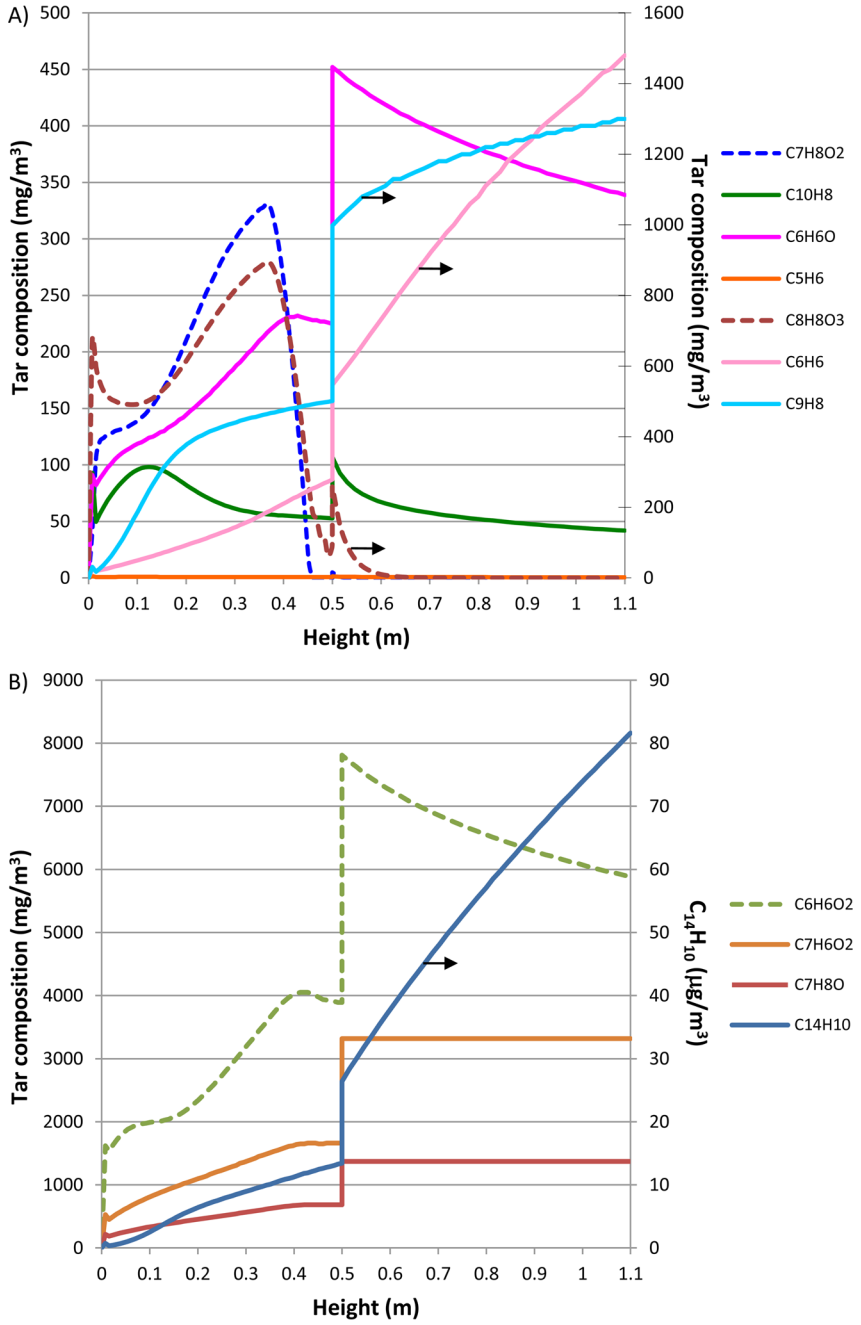

Figure 5. (A and B) Tar composition in the emulsion phase from the kinetic model along the gasifier using an ER value of 0.26.

was established as the one necessary to achieve a carbon conversion of 97%. Allowing the system to higher values of carbon conversion made the model unstable.

From the experimental data it can be inferred that less than 2.6 and 1.8 vol % of the total gases corresponded to the tar fraction for an ER of 0.25 and 0.26, respectively. The compositions of sulfur- and chlorine-containing gases, ammonia, and NO_x were not reported. From the model, 0.9 and 0.6 vol % of the gases were tars for an ER of 0.25 and 0.26, respectively. It was previously reported that the total tar yield decreased from 10.15% to 0.26% of the initial biomass feedstock when the ER value was increased from 0 to 0.34; at ER values greater than 0.34, the benefits of adding more oxygen showed to be reduced.[4] The kinetic model also agrees with the experimental data in that total tar was reduced, falling by 24% in the empirical case and by 34% in the model, when the ER value was raised, from 0.25 to 0.26. Experimental and kinetic model results showed that individual tar class concentrations were reduced with the increase of ER and gasification temperature. Experimental data showed a greater reduction of classes 2 and 3 and phenol than the kinetic model, while the kinetic model decreased greater class 4.

In regard to noncondensable gases, Table 4 shows that the predicted results presented the same trends in the concentration of species for the two compared ER values, especially consistent for some gases, such as CO_2, CO, and H_2. The greatest differences were for nitrogen and water. The experimental report presented the concentrations on a dry basis; nitrogen concentration was given as 51% with a note that this value was estimated based on mass balance and for H_2O of 15.6% as calculated, for an ER value of 0.25. CO_2 composition agreed among the experimental data and kinetic model.

dx.doi.org/10.1021/ef4004297 | *Energy Fuels* 2013, 27, 2693−2702

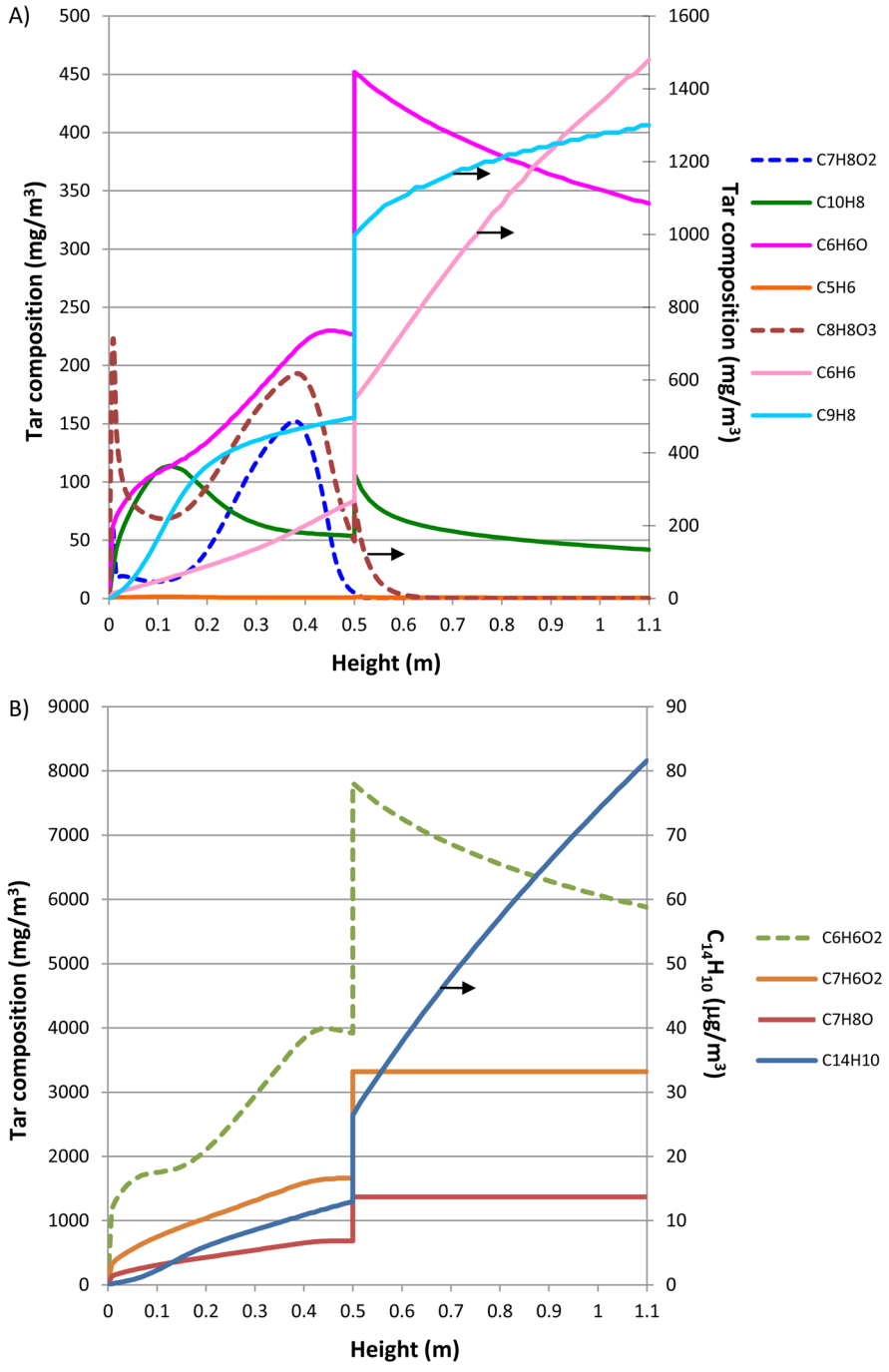

Figure 6. (A and B) Tar composition in the bubble phase from the kinetic model along the gasifier using an ER value of 0.26.

Tar Evolution along the Gasifier Height. Figure 5 shows the composition of tars in the emulsion phase along the gasifier bed and freeboard zone using the kinetic model; for illustration purposes, only the results for an ER value of 0.26 are shown. Primary tars are shown in dashed lines, vanillin ($C_8H_8O_3$) and guaiacol ($C_7H_8O_2$) in Figure 5A and catechol ($C_6H_6O_2$) in Figure 5B. Vanillin and guaiacol were rapidly produced and then destroyed along the bed. At the top of the bed (0.5 m), guaiacol was completely eliminated and vanillin was significantly reduced. In the bed zone, vanillin composition increased in the region between 0.2 and 0.45 m of bed height. This increase or lack of destruction seems to be related to the temperature of the emulsion phase which decreased in this height region (graph not shown) due to less oxygen available.

A very different curve shape can be seen for catechol ($C_6H_6O_2$) in Figure 5B. This is due to catechol being a primary tar and also produced from guaiacol pyrolysis. Catechol concentration increased progressively with height in the bed zone until it reached a maximum and then started decreasing in the freeboard but at a slow rate. Catechol reacted with hydrogen to generate benzene according to reaction R3 and recombined itself to produce naphthalene and phenanthrene in accordance with reactions R5 and R6, respectively. Since the activation energies are relatively high (as shown in Supporting Information), temperatures greater than 1223 K were necessary to decompose catechol into benzene, naphthalene, and phenanthrene, based on the Arrhenius values determined for catechol pyrolysis between 773 and 1273 K by Ledesma et al.[7]

dx.doi.org/10.1021/ef4004297 | *Energy Fuels* 2013, 27, 2693−2702

Figure 6 shows the composition of tars in the bubble phase. The shapes of the curves were very similar to the emulsion phase curves. For vanillin and guaiacol, smaller concentrations are seen as expected, since these two compounds were transferred from the emulsion phase where they were produced.

An abundant secondary tar is phenol (C_6H_6O), which was increasingly produced along the bed, reaching a maximum value of 452 mg/m^3 at the top of the bed. Phenol was considerably reduced in the freeboard zone (above 0.5 m) to a value of 339 mg/m^3.

Another secondary tar is *o*-cresol (C_7H_8O) shown in Figures 5B and 6B. It can be seen that *o*-cresol concentration increased with height and remained constant in the freeboard zone. This is another compound that requires addition of reactions that correspond to *o*-cresol gasification and combustion.

Benzene and indene are considered both secondary and tertiary tars since they often appear in both classes.[2] Figures 5A and 6A show that benzene and indene were formed in the bed and also continued to be generated in the freeboard zone. Reactions R25 and R26 (shown in section 3) correspond to combustion and steam reforming of benzene, respectively. Even though these two reactions were included in the model, benzene concentration increased, which shows that it required more heat to be destroyed because oxygen was limited in the freeboard.

From experimental work on biomass gasification, it has been reported that benzene and naphthalene are two of the aromatic species present in notable amounts. While most aromatic compounds reached a maximum formation at either 1073 or 1173 K, followed by steady destruction with increasing temperature, benzene was one of the most stable one-ring species and was not completely destroyed even at 1473 K.[32]

The presence of cyclopentadiene (C_5H_6) was negligible since it is considered an intermediate compound that was produced by reaction R4 where CO was abstracted from phenol.[33] Once cyclopentadiene was generated it immediately reacted to produce naphthalene according to reaction R7.[19]

Very low concentrations were seen for naphthalene ($C_{10}H_8$) and phenanthrene ($C_{14}H_{10}$) as shown in Figure 6A and 6B, respectively. Oxidation of naphthalene according to reaction R8 was more favorable in the bed zone where oxygen was available. In the freeboard, steam reforming of naphthalene (reaction R24) was more dominant and produced benzene. Phenanthrene was generated mainly in the freeboard at very low concentration (<135 μg/m^3). These results agreed with work on characterization of tars. It was reported that naphthalene was the most quantitatively important tertiary tar analyzed and that PAH compounds were present in insignificant amounts up to temperatures of approximately 1023−1073 K.[2]

It was observed that the increase in temperatures of the bubble and emulsion phases in the bed was caused by the combustion reactions occurring closer to the bottom of the bed due to the presence of oxygen. Until the bed height is 0.4 m or higher, the oxygen content decreased to less than 1% (mol) and leading to complete absence, respectively, as shown in Figure 7.

This section evaluated the kinetic model using experimental data for wood gasification. Our findings showed consistency with what was expected during evolution of primary tars according to experimental work from a previous report. Thus, this model requires knowledge of the lignin content. Measurement of lignin content can be performed by methods based on fractionation of biomass, such as the acid detergent lignin (ADL) method.[10]

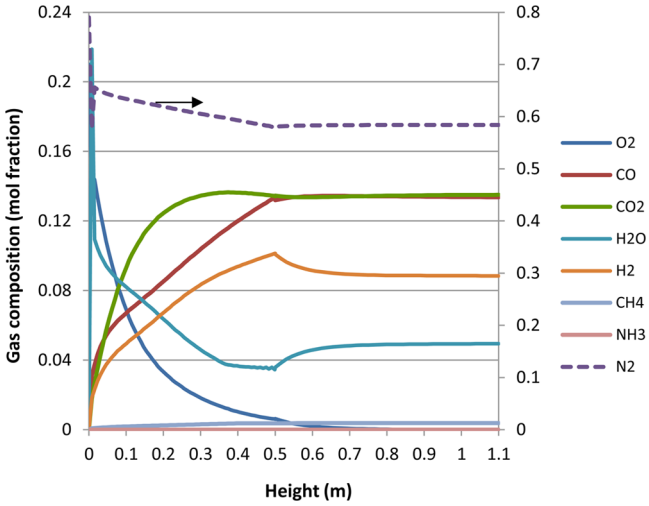

Figure 7. Gases composition in the bubble phase from the kinetic model along the gasifier using an ER value of 0.26.

5. CONCLUSIONS

Tar formation during biomass gasification is a major issue because these byproducts affect the end use of the gasification product, causing problems such as pipeline plugging and damage to gas engines. Therefore, a kinetic model for biomass gasification that incorporated tar formation and evolution was evaluated in this work. The model was verified using experimental data from gasification of beech. Since lignin was assumed as the main precursor of tars formation, the lignin content of biomass was required as part of the fuel characterization. The kinetic model results showed consistency with what is expected during evolution of primary tars according to experimental work from previous reports. However, the model overestimated the total tar concentration and tars of class 2. Moreover, the kinetic model has the additional benefit of providing information on formation of tars and their behavior when the ER value was raised. The model showed that the most abundant tar compounds were catechol, *o*-cresol, and salicylaldehyde, which require further experimental studies to obtain kinetic parameters for their pyrolysis and gasification, since kinetic data for their destruction was not available for inclusion in the model. The completeness of the kinetics would improve the fidelity of the tar simulation, which would help future research.

■ ASSOCIATED CONTENT

Supporting Information

Appendix A: Equations of mass and energy balances for the emulsion phase, bubble phase, carbonaceous material, and freeboard zone. Appendix B: Thermodynamic analysis of possible reactions. Appendix C: Kinetic parameters for all the reactions (as shown in Table 1) involved in the kinetic model. This material is available free of charge via the Internet at http://pubs.acs.org.

■ AUTHOR INFORMATION

Corresponding Author

*Phone: +44(0) 113 343 9010. E-mail: C.FontPalma@leeds.ac.uk; c.fontpalma@gmail.com.

Present Address

[†]Energy Technology and Innovation Initiative, University of Leeds, Leeds, United Kingdom, LS2 9JT.

Notes

The authors declare no competing financial interest.

■ ACKNOWLEDGMENTS

The author would like to thank the National Council on Science and Technology (CONACYT) of Mexico for their financial support.

■ REFERENCES

(1) Devi, L.; Ptasinski, K. J.; Janssen, F. J. J. G. *Biomass Bioenergy* **2003**, *24*, 125−140.
(2) Morf, P.; Hasler, P.; Nussbaumer, T. *Fuel* **2002**, *81*, 843−853.
(3) Fourcault, A.; Marias, F.; Michon, U. *Biomass Bioenergy* **2010**, *34*, 1363−1374.
(4) Su, Y.; Luo, Y.; Chen, Y.; Wu, W.; Zhang, Y. *Fuel Process. Technol.* **2011**, *92*, 1513−1524.
(5) Faravelli, T.; Frassoldati, A.; Migliavacca, G.; Ranzi, E. *Biomass Bioenergy* **2010**, *34*, 290−301.
(6) Fitzpatrick, E. M.; Bartle, K. D.; Kubacki, M. L.; Jones, J. M.; Pourkashanian, M.; Ross, A. B.; Williams, A.; Kubica, K. *Fuel* **2009**, *88*, 2409−2417.
(7) Ledesma, E. B.; Marsh, N. D.; Sandrowitz, A. K.; Wornat, M. J. *Energy Fuels* **2002**, *16*, 1331−1336.
(8) Swierczynski, D.; Courson, C.; Kiennemann, A. *Chem. Eng. Process.* **2008**, *47*, 508−513.
(9) Devi, L.; Ptasinski, K. J.; Janssen, F. J. J. G. *Fuel Process. Technol.* **2005**, *86*, 707−730.
(10) Font Palma, C. Modelling of tar formation and evolution for biomass gasification: A review. *Appl. Energy* submitted for publication.
(11) McKendry, P. *Bioresour. Technol.* **2002**, *83*, 37−46.
(12) Hosoya, T.; Kawamoto, H.; Saka, S. *J. Anal. Appl. Pyrol.* **2008**, *83*, 78−87.
(13) Adler, E. *Wood Sci. Technol.* **1977**, *11*, 169−218.
(14) Radmanesh, R.; Chaouki, J.; Guy, C. *AIChE J.* **2006**, *52*, 4258−4272.
(15) Di Blasi, C. *Prog. Energy Combust. Sci.* **2008**, *34*, 47−90.
(16) Shin, E.-J.; Nimlos, M. R.; Evans, R. J. *Fuel* **2001**, *80*, 1689−1696.
(17) Wahyudiono; Kanetake, T.; Sasaki, M.; Goto, M. *Chem. Eng. Technol.* **2007**, *30*, 1113−1122.
(18) Sharma, R. K.; Hajaligol, M. R. *J. Anal. Appl. Pyrol.* **2003**, *66*, 123−144.
(19) Marinov, N. M.; Pitz, W. J.; Westbrook, C. K.; Castaldi, M. J.; Senkan, S. M. *Combust. Sci. Technol.* **1996**, *116*, 211−287.
(20) Norinaga, K.; Deutschmann, O.; Saegusa, N.; Hayashi, J.-i. *J. Anal. Appl. Pyrol.* **2009**, *86*, 148−160.
(21) Petersen, I.; Werther, J. *Chem. Eng. Process.* **2005**, *44*, 717−736.
(22) Corella, J.; Sanz, A. *Fuel Process. Technol.* **2005**, *86*, 1021−1053.
(23) Chan, W.-C. R.; Kelbon, M.; Krieger, B. B. *Fuel* **1985**, *64*, 1505−1513.
(24) Gerber, S.; Behrendt, F.; Oevermann, M. *Fuel* **2010**, *89*, 2903−2917.
(25) Tinaut, F. V.; Melgar, A.; Perez, J. F.; Horrillo, A. *Fuel Process. Technol.* **2008**, *89*, 1076−1089.
(26) Chejne, F.; Lopera, E.; Londoño, C. A. *Fuel* **2011**, *90*, 399−411.
(27) Andersen, J.; Jensen, P. A.; Hvid, S. r. L.; Glarborg, P. *Energy Fuels* **2009**, *23*, 5783−5791.
(28) Verdone, N.; De Filippis, P. *Chem. Eng. Sci.* **2006**, *61*, 7487−7496.
(29) Jess, A. *Fuel* **1996**, *75*, 1441−1448.
(30) Kiel, J. H. A.; van Paasen, S. V. B.; Neeft, J. P. A.; Devi, L.; Ptasinski, K. J.; Janssen, F. J. J. G.; Meijer, R.; Berends, R. H.; Temmink, H. M. G.; Brem, G.; Padban, N.; Bramer, E. A. Primary measure to reduce tar formation in fluidised-bed biomass gasifiers. *Final Report SDE project P1999-012*; Agency for Research in Sustainable Energy: Petten, The Netherlands, March 2004.
(31) Han, J.; Kim, H. *Renewable Sustainable Energy Rev.* **2008**, *12*, 397−416.
(32) Zhang, Y.; Kajitani, S.; Ashizawa, M.; Oki, Y. *Fuel* **2010**, *89*, 302−309.
(33) Cypres, R.; Bettens, B. *Tetrahedron* **1974**, *30*, 1253−1260.